Journal of Theoretical and Applied Information Technology
10th March 2013. Vol. 49 No.1

ISSN: 1992-8645 www.jatit.org E-ISSN: 1817-3195

SPATIOTEMPORAL DYNAMICS OF NDVI AND LAND USE IN CHINA BASED ON REMOTE SENSING IMAGES

[1]YAPING ZHANG, [2]ZHENPING QIANG, [2]XU CHEN
[1] School of Information Science and Technology, Yunnan Normal University, Kunming, China
[2]Computer & Information Science Department, Southwest Forestry University, Kunming, China
E-mail: [1]zhangyp.cs@gmail.com, [2]chenxu_gis@yahoo.com.cn

ABSTRACT

Using the fuzzy rule-based classification method, seventeen phases of NDVI (Normalized Difference Vegetation Index) images acquired from 1982 to 1998 were classified respectively based on NDVI and climate images. And then, spatiotemporal dynamics of NDVI and land use are described. Finally, this paper analyzes NDVI trends and their relationships with climate and human activity under the land cover scenario. The results indicate that at the national scale, the increases of monthly and seasonal NDVI correspond mainly to climate changes. But NDVI trends show a large spatial and temporal heterogeneity at the regional scale corresponding mainly to human activities, besides some sensitive areas with climate changes. Therefore it is necessary to establish a set of policies to ensure the ecological conservation and restoration, especially in ecological sensitivity areas.

Keywords: *NDVI, Spatiotemporal Dynamics, Time-Series*

1. INTRODUCTION

Normalized Difference Vegetation Index (NDVI) is a general biophysical parameter that correlates with photosynthetic activity of vegetation and provides an indication of the 'greenness' of the vegetation [1]. It is calculated as NDVI = (CH2−CH1) / (CH2+CH1) usually, where CH1 and CH2 represent radiances from channels 1 (0.58–0.68 mm) and 2 (0.725–1.10 mm) of the AVHRR, respectively. NDVI does not provide land cover type directly. However, a time series of NDVI values can separate different land cover types based on their phenology, or seasonal signals [2]. Time series of continuous Earth Observation (EO) based estimates of vegetation have significantly improved our understanding of intra and inter-annual variations in vegetation from a regional to global scale [3]. Different global coverage products based on AVHRR data have been used for numerous regional to global scale vegetation studies. For example, lots of studies analyse the AVHRR NDVI time series from regional to global scale [4-5] and changes in vegetation phenology [6-7] based on NDVI. Furthermore, long term time series analysis of AVHRR NDVI have been intercompared with other climatic variables like rainfall and air temperature to reveal geo-biophysical causes for observed changes in vegetation greenness or NPP [8-9]. Other geophysical parameters like albedo have been derived from Meteosat data [10] to analyse continental scale trends associated with environmental changes.

China's geographic size causes the country to have a large climate range, from the tropical to subarctic/alpine and from rain forest to desert, together with diverse and species-rich vegetation types. It is necessary to pay enough attention to land cover monitoring and land use planning, so as to protect natural environment and ecosystem effectively [11]. Land use patterns have been dramatically changed in China since the late 1980s, especially with regard to urbanization and loss of cultivated land. The large scale land use change in China over the last two decades of the 20th century has attracted international attention to analyze the driving forces, impacts and future trends [12]. In the late 20th century and early 21st century, China has undergone a rapid socio-economic development, modification of industrial structure and acceleration of industrialization and urbanization. Meanwhile, a series of development strategies, including "Western Development", "Revitalization of Northeast", "Rising of Central China" and so on have been implemented across the nation. It results in remarkable changes and modifications in the spatial distribution of China's land use [13]. In this paper, we used the NDVI data from 1982 to 1998, to gather with information on climate and land use, to explore interannual variations of monthly and

ISSN: 1992-8645 www.jatit.org E-ISSN: 1817-3195

seasonal NDVI and their relationships with climate and human activity.

2. RESEARCH METHOD

2.1 Data

The Normalized Difference Vegetation Index (NDVI) data used in this study were derived from the NOAA/AVHRR Land data set by the Global Inventory Monitoring and Modeling Studies (GIMMS) group; its spatial resolution was 8×8 km^2 with 15-day intervals, between January 1982 and December 1998 [14-16]. Annual mean air temperature and precipitation data at 1×1 km^2 resolution were compiled from the 1982–1998 temperature/precipitation database of China. Available data and maps for this study include: (a). Land Use Map of China (1:1,000,000), edited by the Editorial Committee for the 1:1,000,000 Land Use Map of China, published by Science Press, Beijing, 1990; (b). Resources and environment data of China (1:4,000,000), produced by the State Key Laboratory of Resources and Environment Information Systems of the Institute of Geography, at the Chinese Academy of Sciences, Beijing November 1996. The data include 13 specific datasets: national boundaries, provincial boundaries, county boundaries, canals, railway system, rivers, main road system, and surface waters etc; (c). DEM of GTOPO30 that USGS distributes to the public through the Internet ; (d). Land Use Map of China in 1995 from sharing infrastructure of Earth system science. All data were aggregated to grid cells at 8×8 km^2 resolution, as done for the NDVI data sets. And then, the mask, geometric correction, coordination transformation, and layer stack were carried out on images with ArcGIS 9.3.

2.2 Method

As some variations (clouds, aerosols, etc) may still remain in the GIMMS NDVI data, the mean-value iteration filter (MVI) [17] was conducted to reconstruct a high quality NDVI time-series and to support a multi-temporal analysis for 15-day interval NDVI data sets from 1982 to 1998. To further reduce residual atmospheric and bidirectional effect, the maximum NDVI values in each season and year were produced from the seasonal and annual NDVI data sets [18].

There exist different uncertainties in many real world applications and the fuzzy technique has been witnessed to be a powerful modeling tool to these uncertainties [19-20]. Usually only fuzzy concepts exist for land cover and land use. Hence, fuzzy classification systems, such as fuzzy c-means clustering algorithm [21], are well suited to handle most sources of vagueness in remote sensing information extraction. Fuzzy logic is a multi-valued logic quantifying uncertain statements. It can model imprecise human thinking and can represent linguistic rules [22]. Fuzzy classification systems consist of three main steps: fuzzification, the combination of fuzzy sets (e.g. by fuzzy rule), and defuzzification. Fuzzy rules are ‘‘if–then’’ rules. If a condition is fulfilled, an action takes place. An example is: ‘‘If’’ feature x is low, ‘‘then’’ the image object should be assigned to land cover W. In fuzzy terminology this would be written: If feature x is a member of fuzzy set low, then the image object is a member of land cover W [22]. According to the land use/cover categories suggested by the Chinese Academy of Sciences, the land use/cover types in this study were classified as: Farmland, Forestland, Grassland, Water Area, Urban Land, and Unused Land. Then annual fuzzy rules were extracted from seasonal NDVI, annual NDVI, temperature, precipitation and DEM images, respectively, in reference to the Land Use Map of China 1:1,000,000. For example, if all five of these variables are in their respective fuzzy set low, then the image object is a member of land cover Unused Land. Using these fuzzy rules assembled for every year, seventeen land use-classified maps were obtained, one for each year from 1982 to 1998 (Figure 1).

3. RESULTS AND DISCUSSION

3.1 Fuzzy classification accuracy

Based on the reference of the Land Use Map of China, Kappa coefficients of all classified images were very high and gradually decreased from 94.05% in 1982 to 92.46% in 1998 (Figure 2). The maximum Kappa coefficient value was 96.65% in 1991 and the minimum value was 91.74% in 1983. If three outlying years (1983, 1991 and 1997) are ignored, the values from 1982 to 1998 decrease significantly (r^2 = 0.329, p = 0.0321) with a trend of -0.000617 yr^{-1} (Figure 2). These figures imply that the change of land use in China is getting extreme.

Journal of Theoretical and Applied Information Technology
10th March 2013. Vol. 49 No.1

ISSN: 1992-8645 www.jatit.org E-ISSN: 1817-3195

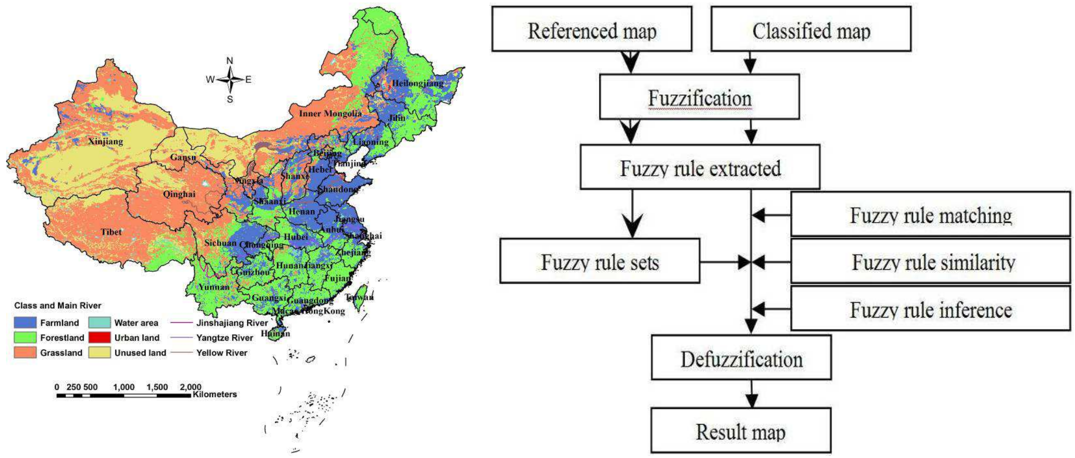

(a) Land Use Map of China (b) Classification flow diagrams

Figure 1. Land Use Map Of China Referenced And Fuzzy Rule-Based Classification Flow Diagrams.

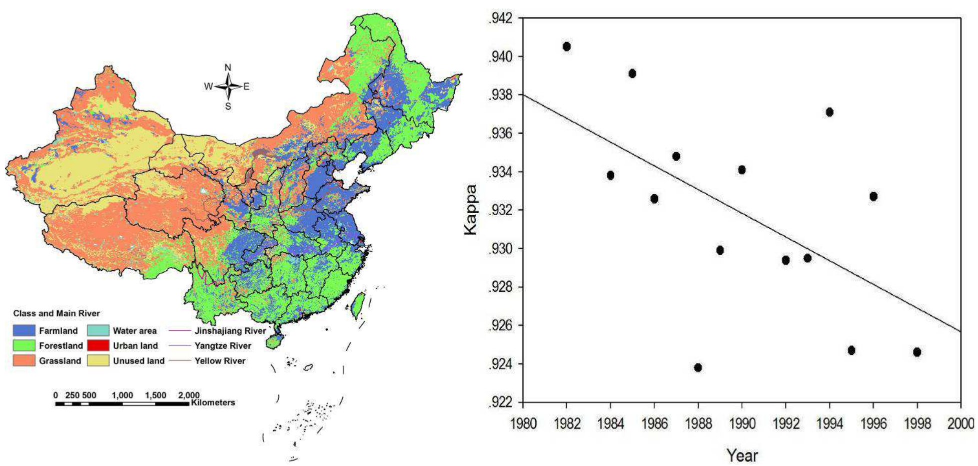

(a) Classified image of China in 1998 (b) Kappa values trend

Figure 2. Classified Image Of China In 1998 And Kappa Values Trend From 1982 To 1998

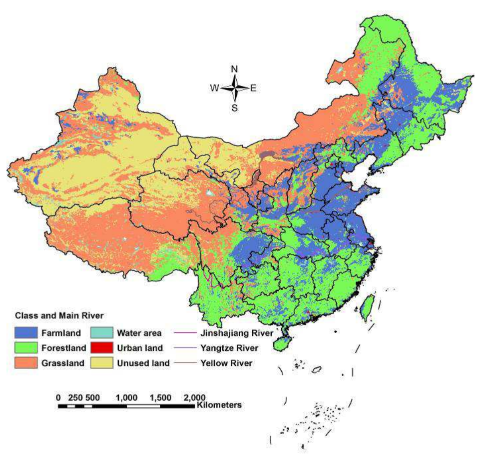

Figure 3. Land Use Map Of China In 1995

Based on the Land Use Map of China in 1995 (Figure 3), the Kappa coefficient of classified image 1995 was 80%, and the overall accuracy and mean accuracy were 85% and 81.2% respectively

Journal of Theoretical and Applied Information Technology
10th March 2013. Vol. 49 No.1

ISSN: 1992-8645 www.jatit.org E-ISSN: 1817-3195

(Table 1). It can be seen that 88.5% of the actual Forestland pixels (34460 out of 38933) were correctly identified; the producer of the map incorrectly omitted 11.5% of the pixels (4473 out of 38933). Looking at the columns, we can see that 87.6% of the Forestland pixels (34460 out of 39332) were correctly identified and 4872 out of 39332 or 12.4% of the Forestland pixels were incorrectly assigned to other classes during the classification process (Table 1). Water Area shows a lower degree of accuracy. Water areas are not spectrally homogeneous or distinct since they contain wetlands and aquatic plants, as well as other land covers in an 8×8 km^2 pixel. For this reason, there is some spectral confusion with the other classes in the matrix.

Table 1. Land Use Types Error Matrix Between 1995R (Reference Data) And 1995C (Classified Data) (Pixels) and Kappa value

1995C / 1995R	Farm land	Forest land	Grass land	Water Area	Urban Land	Unused Land	Row Total	Producer's Accuracy	Errors of Omission
Farmland	25558	2292	1659	46	52	309	29916	85.4%	14.6%
Forestland	1378	34460	2649	37	10	399	38933	88.5%	11.5%
Grassland	1165	2031	40034	115	6	5252	48603	82.4%	17.6%
Water Area	185	78	217	1572	12	132	2196	71.6%	28.4%
Urban Land	27	19	8	2	181	7	244	74.2%	25.8%
Unused Land	580	452	2843	187	1	23469	27532	85.2%	14.8%
Column Total	28893	39332	47410	1959	262	29568	147424		
User's Accuracy	88.5%	87.6%	84.4%	80.2%	69.1%	79.4%			
Errors of Commission	11.5%	12.4%	15.6%	19.8%	30.9%	20.6%			
Kappa value	Kappa=80%								

Overall Accuracy = 85%, Mean Accuracy = 81.2%

3.2 Spatiotemporal Dynamics of Land Use

The main spatial distribution changes of land cover type in 1982-1998 existed in the reaches of the Yangtze River and the Yellow River, central Shandong and Guizhou, southern Inner Mongolia, eastern Tibet, northern Xinjiang, in most parts of Qinghai, Sichuan, Yunnan and Hunan (Figure 4(a)). The areas of farmland, water area, urban land and unused land increased; water area had the greatest rate of increase, which was 8.52% during the period. The areas of forestland and grassland decreased; forestland had the biggest rate of decrease, which was 1.56% during the period. The main characteristics of the change in land cover types over the period 1982-1998 are detailed in Figure 4(b) and Table 2.

(1) Although 1182.08×10^4 and 404.48×10^4 hectares of farmland were converted into forestland and grassland respectively, the area of farmland increased by 379.52×10^4 hectares. The net increase was mainly derived from the occupation of forestland (1459.84×10^4 hectares), and grassland (547.84×10^4 hectares). Forest loss occurred primarily in southern and eastern China, such as the lower reaches of Yellow River, the Yangtze River Basin, Yunnan, Guizhou, Sichuan, Guangdong, Fujian, Shaanxi, and Shandong Provinces. Similarly, the farmland converted into forestland also occurred primarily in these regions. The occupation of grassland by farmland was mainly distributed in Inner Mongolia, the Yellow River Basin and central Tibet. Farmland converted into grassland was also mainly found in these regions except Inner Mongolia.

(2) Overall the area of forestland decreased by 382.72×10^4 hectares. Increases in forestland were mainly attributed to the occupation of farmland (1182.08×10^4 hectares) and grassland (545.28×10^4 hectares). However 1459.84×10^4 hectares and 564.48×10^4 hectares of forestland were converted into farmland and grassland respectively, which resulted in net losses to these groups. In addition, 304.64×10^4 hectares of forestland was converted into unused land and only 238.72×10^4 hectares was conversely converted. The conversion between forestland and other land cover types occurred mainly in central, southern and eastern

Journal of Theoretical and Applied Information Technology
10th March 2013. Vol. 49 No.1

ISSN: 1992-8645 www.jatit.org E-ISSN: 1817-3195

China, Inner Mongolia, and the southeastern Qinghai-Tibet Plateau.

(3) There was a decrease of 466.56×10^4 hectares in grassland which was the most dominant conversion during the study period. The decrease of grassland mainly derived from the occupation of unused land (963.2×10^4 hectares), farmland (547.84×10^4 hectares) and water area (131.2×10^4 hectares). Conversely, 720×10^4 hectares, 404.48×10^4 hectares and 30.72×10^4 hectares of unused land, farmland and water were converted into grassland respectively. Grassland was converted into water bodies mainly in eastern Xinjiang, northwestern Qinghai and Shanxi, and the southeastern portions of the Qinghai-Tibet Plateau and Inner Mongolia Autonomous Region. The conversion between grassland and unused land is particularly evident in the middle and upper reaches of the Yellow River, Inner Mongolia, Gansu and northwestern Qinghai. Additionally, some conversions were distributed in the eastern Qinghai-Tibet Plateau and northern Xinjiang.

(4) Water area increased by 112.64×10^4 hectares over the study period. Besides grassland, the second source of conversion to water was forestland (33.28×10^4 hectares), this mainly distributed in eastern Jiangxi Province and northern Guangdong Province.

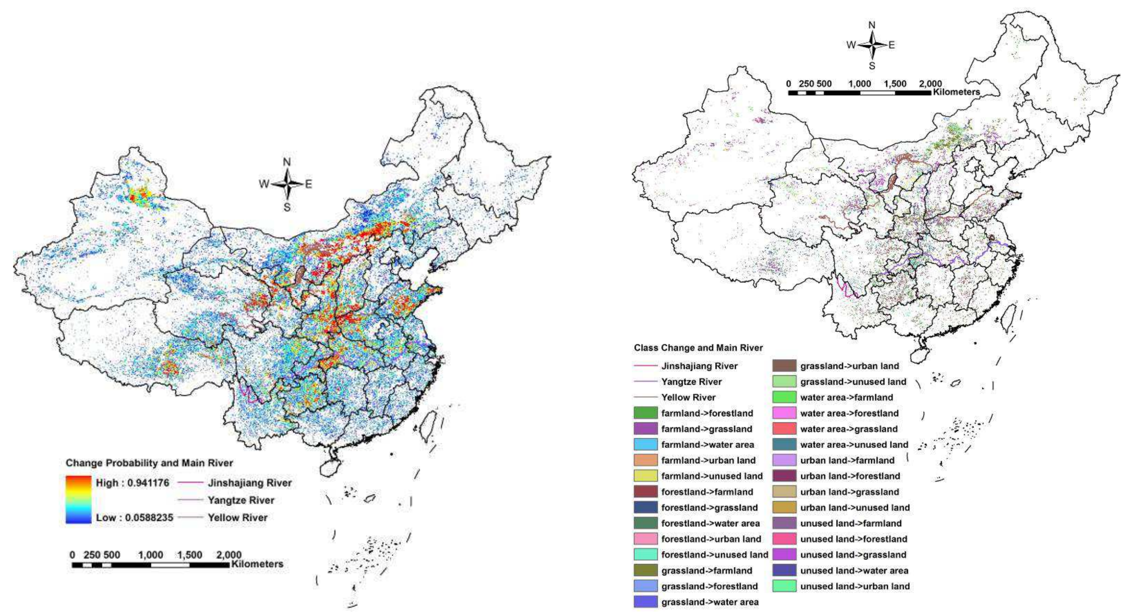

(a) Change probability (b) Land cover types change in 1982-1998

Figure 4. Mainly Spatial Distributions Of Land Cover Types Change During 1982-1998

Table 2. Land Use Types Transformation Matrix From 1982 To 1998 (10^4 Hectares)

1998 / 1982	Farmland	Forestland	Grassland	Water area	Urban land	Unused land	total
Farmland	17002.88	1182.08	404.48	5.12	9.60	339.20	18943.36
Forestland	1459.84	22236.8	564.48	33.28	3.84	304.64	24602.88
Grassland	547.84	545.28	29720.96	131.20	1.92	963.20	31910.40
Water area	10.24	14.08	30.72	1242.24	0.00	24.96	1322.24
Urban land	2.56	3.20	3.20	0.00	141.44	1.92	152.32
Unused land	299.52	238.72	720.00	23.04	5.12	16149.76	17436.16
Total	19322.88	24220.16	31443.84	1434.88	161.92	17783.68	94367.36
increasing rate	2.00%	-1.56%	-1.46%	8.52%	6.30%	1.99%	

(5) Urban land increased by 9.6×10^4 hectares, but it had the second greatest positive rate of increase, of 6.3%, during the study period. The increase of urban land primarily came at the expense of

Journal of Theoretical and Applied Information Technology
10th March 2013. Vol. 49 No.1

ISSN: 1992-8645 www.jatit.org E-ISSN: 1817-3195

farmland (7.04×10^4 hectares) and distributed around the border area of Hebei and Shandong Provinces, as well as in Qinghai Province.

(6) Unused land increased by 347.52×10^4 hectares and had a similar rate to farmland. Its increase came primarily at the expense of grassland (243.2×10^4 hectares), forestland (65.92×10^4 hectares) and farmland (39.68×10^4 hectares). The conversion to unused land from farmland occurred primarily in the middle and lower reaches of the Yangtze River and the Yellow River Basin, as well as in southern Inner Mongolia, Shaanxi, Shanxi, Henan, Shandong, and Ningxia. The reverse conversion of unused land into farmland occurred mainly in the middle and lower reaches of the Yellow River and Xinjiang.

3.3 Spatiotemporal Dynamics of NDVI

3.3.1 Temporal dynamics of NDVI in national scale

From 1982 to 1998, there was not a significant correlation between annual mean NDVI and climatic factors, and no apparent trend was seen in annual NDVI ($r^2 = 0.123$, $p = 0.169$). But the NDVI trends for spring and autumn increased significantly. The largest NDVI increase ($r^2 = 0.533$, $p = 0.001$) was in spring, with a magnitude of 17.7% over the 17 years and a trend of 0.00211 yr^{-1} (the 17-year averaged NDVI is 0.3111). The increase ($r^2 = 0.355$, $p = 0.012$) for autumn was 7.21% with a trend of 0.001126 yr^{-1}. Despite the pronounced NDVI increases in two seasons, several large fluctuations appeared in the NDVI trends. For example, seasonal NDVI was large in 1987 and 1990 but small in 1991 and 1995 for spring and autumn respectively (Figure 5(a)).

The magnitude of monthly NDVI and its change over time are important indicators of the contribution of vegetation activity in different months to annual plant growth total [16]. In China, the monthly NDVI trends showed positive values for all months except November and December, indicating that NDVI increased throughout the year almost over the 17-year study period (Figure 5(b)). The monthly NDVI trends for May and September increased significantly. The largest monthly NDVI increase ($r^2 = 0.531$, $p = 0.001$) was in May, with a magnitude of 19.96% over the 17 years and a trend of 0.0022 yr^{-1} (the 17-year averaged NDVI is 0.3047). The increase ($r^2 = 0.358$, $p = 0.011$) for September was 8.14% with a trend of 0.001243 yr^{-1}. But monthly NDVI reached maximum value in August and was rather small from December through March (Figure 5(b)). That is, plant growth peaked in the middle of growing season (summer), while the largest NDVI increase occurred in the early growing season (spring). Monthly and seasonal NDVI trends and their patterns are likely coupled with climate patterns and moisture availability [16].

3.3.2 Temporal dynamics of NDVI in provincial scale

Although no apparent trend was seen in annual NDVI at the national scale from 1982 to 1998, we found a high degree of spatial heterogeneity in most areas, especially in the North China Plain, hilly and plain areas of Central China, Yangtze River deltas and Pearl River deltas. At the provincial scale, the provincial NDVI trends for Inner Mongolia ($r^2 = 0.235$, $p = 0.049$), Shanxi ($r^2 = 0.378$, $p = 0.009$), Xinjiang ($r^2 = 0.339$, $p = 0.014$) and Ningxia ($r^2 = 0.292$, $p = 0.025$) increased significantly. The largest provincial NDVI increase was in Ningxia, with a magnitude of 42.59% over the 17 years and a trend of 0.002943 yr^{-1} (the 17-year averaged NDVI was 0.323). The increase for Inner Mongolia, Shanxi and Xinjiang were 7.22%, 10.76%, and 17.61% with a trend of 0.001908 yr^{-1}, 0.002613 yr^{-1}, and 0.001322 yr^{-1}, respectively. But because a rapid urbanization had taken place over the past 20 years, there was significantly decrease in Guangdong ($r^2 = 0.27$, $p = 0.032$), with a trend of -0.001845 yr^{-1}.

3.3.3 Temporal dynamics of NDVI in Land use scale

Similar to annual NDVI and its trend over the past 17 years at the provincial scale, if we assumed the location of land cover was not change in Land Use Map of China referenced (Figure 1(a)), annual NDVI and its trends showed a high degree of heterogeneity at land cover scale. Especially, the annual NDVI trends increased significantly for water area ($r^2 = 0.254$, $p = 0.039$) with a magnitude of 12.18% over the 17 years and a trend of 0.001295 yr^{-1} (Table 3). Compare with spatiotemporal dynamics of land use from 1982 to 1998 (Figure 4 and Table 2), regional NDVI trends and their patterns are likely associated with human activities because of land use changed significantly.

Journal of Theoretical and Applied Information Technology
10th March 2013. Vol. 49 No.1

ISSN: 1992-8645 www.jatit.org E-ISSN: 1817-3195

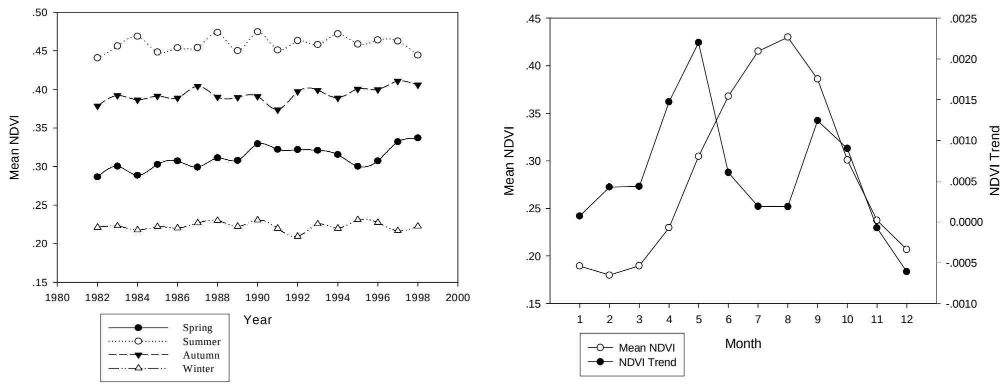

(a) Seasonal NDVI (b) Monthly NDVI

Figure 5. Seasonal And Monthly NDVI Change In China

Table 3. NDVI Regression Analysis From 1982 To 1998 In Land Use Scale

Landuse	N	Reg Coef	T	P	R	I rate
Farmland	17	0.001482	2.003	.064	.459	0.064469
Forestland	17	-0.000373	-.671	.512	.171	-0.02506
Grassland	17	0.001004	1.807	.091	.423	0.053312
Water area	17	0.001295	2.259	.039	.504	0.121757
Urban land	17	-0.000344	-.389	.703	.100	0.046945
Unused land	17	0.000606	1.720	.106	.406	0.105325

3.4 Discussion

A comparison of the NDVI trends in China resulting from this analysis with those found in other studies provides context and support for the overall results of the present study. Reference [16] used the NDVI data from 1982 to 1999, together with information on climate, vegetation, and human activity, to explore interannual variations of monthly and seasonal NDVI and their relationships with climate and land use change. At the national scale, they found that monthly and seasonal NDVI had increased significantly over the study period and NDVI had showed the largest increase (14.4% during the 18 years and a trend of 0.0018 yr^{-1}) over 85.9% of the total study area in spring and the smallest increase (5.2% with a trend of 0.0012 yr^{-1}) over 72.2% of the area in summer, while the NDVI trends had showed a marked heterogeneity corresponding to regional and seasonal variations in climates. The results were very similar to our analysis in this paper. But in this study, NDVI in summer did not appear the significant change and monthly NDVI trend was negative values for November (Figure 5(b)). Because reference [16] not only assume that such variations were smaller than those due to environmental drivers, and grid cells with <0.1 of annual average NDVI during 18 years were excluded to reduce the influence of soil (over deserts and sparsely vegetated grids) and snow on the NDVI trend, but also aggregated monthly NDVI to grid cells of 0.1°× 0.1° from the original 8-km resolution data. However, in this study, the mean-value iteration filter (MVI) [17] was used to reduce the noise and reconstruct the high quality NDVI time-series. These differences of NDVI data preprocess would cause slight bias in some results.

4. CONCLUSION

The multiyear NDVI data set and a corresponding climate data set from 1982 to 1998 were used to analyze NDVI trends and their relationships with climate and human activity. The results indicated that both increase of monthly and seasonal NDVI corresponded mainly to climate changes, suggesting that climate change is playing an important role for the patterns of NDVI trends at the national scale. But NDVI trends showed a large spatial and temporal heterogeneity at the regional scale corresponding mainly to human activities, suggesting that human activities is playing an important role for the patterns of NDVI trends at the regional scale, besides some sensitive areas with

ISSN: 1992-8645 www.jatit.org E-ISSN: 1817-3195

climate changes. Human activities have exerted a large effect on the spatiotemporal patterns of NDVI trends in some regions. If human activities would exceed regulation capacity of ecosystems themselves, the ecosystems in China might be deteriorated more seriously. It is necessary to establish a set of policies to ensure the ecological conservation and restoration, especially in ecological sensitivity areas.

ACKNOWLEDGEMENTS

This work was financially supported by applied basic research programs of Yunnan Province (2010CD047) and (2011FZ140).

REFRENCES:

[1] P. J. Sellers, "Canopy reflectance, photosynthesis, and transpiration", International Journal of Remote Sensing, vol. 6, 1985, pp. 1335–1372.

[2] M. P. Lenney, C. E. Woodcock, and J. B. Collins, "The status of agricultural lands in Egypt: the use of multitemporal NDVI features derived from Landsat TM", Remote Sensing of Environment, vol. 56, 1996, pp. 8–20.

[3] R. Fensholt, K. Rasmussen, T. T. Nielsen, and C. Mbow, "Evaluation of earth observation based long term vegetation trends — Intercomparing NDVI time series trend analysis consistency of Sahel from AVHRR GIMMS, Terra MODIS and SPOT VGT data", Remote Sensing of Environment, Vol. 113, No. 9, 2009, pp. 1886-1898.

[4] A. Anyamba and C. J. Tucker, "Analysis of Sahelian vegetation dynamics using NOAA AVHRR NDVI data from 1981–2003", Journal of Arid Environments, vol. 63, 2005, pp. 596−614.

[5] A. T. Jeyaseelan, P. S. Roy, and S. S. Young, "Persistent changes in NDVI between 1982 and 2003 over India using AVHRR GIMMS (Global Inventory Modeling and Mapping Studies) data", International Journal of Remote Sensing, vol. 28, No. 21, 2007, pp. 4927−4946.

[6] R. Stöckli and P. L. Vidale, "European plant phenology and climate as seen in a 20- year AVHRR land surface parameters data set", International Journal of Remote Sensing, vol. 25, No. 17, 2004, pp. 3303−3330.

[7] B. W. Heumann, J. W. Seaquist, L. Eklundh, and P. Jonsson, "AVHRR derived phenological change in the Sahel and Soudan, Africa, 1982–2005", Remote Sensing of Environment, vol. 108, No. 4, 2007, pp. 385−392.

[8] J. Xiao and A. Moody, "Geographic distribution of global greening trends and their climatic correlates: 1982 to 1998" International Journal of Remote Sensing, vol. 26, No. 11, 2005, pp. 2371−2390.

[9] T. Hickler, L. Eklundh, J. Seaquist, B. Smith, J. Ardö, L. Olsson, M. T. Sykes and M Sjöström, "Precipitation controls Sahel greening trend", Geophysical Research Letters, vol. 32, 2005, pp. L21415.

[10] Y. M. Govaerts and A. Lattanzio, "Estimation of surface albedo increase during the eighties Sahel drought from Meteosat observations", Global and Planetary Change, vol. 64, 2008, pp. 139−145.

[11] X. Chen, R. Tateishi, and C. Wang, "Development of a 1-km landcover dataset of China using AVHRR data", ISPRS Journal of Photogrammetry & Remote Sensing, vol. 54, 1999, pp. 305-316.

[12] J. Zhang and Y. Zhang, "Remote sensing research issues of the National Land Use Change Program of China", ISPRS Journal of Photogrammetry & Remote Sensing, vol. 62, 2007, pp. 461-472.

[13] J. Liu, Z. Zhang, and X. Xu, "Spatial patterns and driving forces of land use change in China during the early 21st Century", Journal of Geographical Sciences, vol. 20, 2010, pp. 483-494.

[14] C. J. Tucker, D. A. Slayback, and J. E. Pinzon, "Higher northern latitude NDVI and growing season trends from 1982 to 1999", International Journal of Biometeorology, vol. 45, 2001, pp. 184–190.

[15] L. M. Zhou, C. J. Tucker, and R. K. Kaufmann, "Variations in northern vegetation activity inferred from satellite data of vegetation index during 1981 to 1999", Journal of Geophysical Research, vol. 106, 2001, pp. 069–083.

[16] S. Piao, J. Fang, L. Zhou, Q. Guo, M. Henderson, W. Ji, Y. Li, and S. Tao, "Interannual variations of monthly and seasonal normalized difference vegetation index (NDVI) in China from 1982 to 1999", Journal of Geophysical Reseach, vol. 108, 2003, pp. 4401.

[17] M. Ma and F. Veroustraete, "Reconstructing pathfinder AVHRR land NDVI timeseries data for the Northwest of China", Advances in Space Research, vol. 37, 2006, pp. 835−840.

ISSN: 1992-8645 www.jatit.org E-ISSN: 1817-3195

[18] B. N. Holben, "Characteristics of maximum value composite images from temporal AVHRR data", International Journal of Remote Sensing, vol. 7, 1986, pp. 1417– 1434.
[19] Y. Li and W. Huang, "A probabilistic fuzzy set for uncertainties-based modeling in logistics manipulator system", Journal of Theoretical and Applied Information Technology, Vol. 46, No. 2, December 2012, pp. 977-982.
[20] W. Huang and Y. Li, "Bell-shaped probabilistic fuzzy set for uncertainties modeling", Journal of Theoretical and Applied Information Technology, Vol. 46, No. 2, December 2012, pp. 875-882.
[21] X. Guan, G. Meng and C. Zhao, "Manufacturing resources classification based on fuzzy clustering algorithm", Journal of Theoretical and Applied Information Technology, Vol. 46, No. 2, December 2012, pp. 632-637.
[22] U. BENZ, P. HOFMANN, G. WILLHAUCK, I. LINGENFELDER and M. HEYNEN, "Multiresolution, object-oriented fuzzy analysis of remote sensing data for GIS-ready information", ISPRS J. Photogramm, vol. 58, 2004, pp. 239--258.